May, 1991] © *1991 The Chemical Society of Japan* *Bull. Chem. Soc. Jpn.*, ***64***, *1623—1631 (1991)* 1623

Combustion Reactions in Methane–Air Premixed Flames

Seishiro FUKUTANI,* Keizo SAKAGUCHI, Nilson KUNIOSHI, and Hiroshi JINNO[†]
Department of Industrial Chemistry, Faculty of Engineering, Kyoto University,
Yoshida-honmachi, Sakyo-ku, Kyoto 606
[†] Department of Chemistry, Faculty of Science and Engineering,
Sophia University, Kioicho 7-1, Chiyoda-ku, Tokyo 102

(Received February 5, 1991)

A reaction scheme reproducing methane combustion by computer simulation under a wide range of stoichiometric ratio has been proposed and applied to flat methane–air premixed flames to elucidate factors determining their propagation mechanisms and the role of C_2 reaction pathways. Main methane combustion reactions, which progress sequentially from the fuel to carbon dioxide, are inhibited at low temperatures due to retarded production of oxygen atoms which are necessary for the oxidation of methyl radicals. The role of C_2 routes have been investigated by comparison of the results obtained by use of the C_2 scheme and a simplified C_1 scheme. Some of the methyl radicals are once recombined to ethane but most of the produced ethane is dissociated again to methyl via ethyl radicals. Then the C_2 routes work as a temporary storage of species and hinder the main combustion reactions which go through C_1 species.

There are two alternative approaches to study in detail the mechanism of a chemical reaction consisting of many elementary reactions; one of them is an analytical approach where the chemical change is divided into the contribution of each elementary reaction based on the measurements of the temperature, the species concentrations and so on, and the other one is a synthetic approach where the chemical change is constructed step by step with possible elementary reactions. The former is usually used in experimental studies and the latter in computer simulations.

This study has simulated methane–air premixed flames using a detailed reaction scheme to investigate the following two points of methane combustion: Why methane flames propagate according to the thermal theory; and how important is the C_2 routes for methane combustion under various conditions. A simplified reaction scheme has also been proposed and used to estimate the second point.

Simulation Model

We used the same assumptions as those described in a previous work[1)] in constructing the simulation model, and obtained the following governing equations for flat flames:

$$\frac{\partial \rho}{\partial t} + \frac{\partial}{\partial x}(\rho v) = 0 \tag{1}$$

$$\frac{\partial}{\partial t}(c_p \rho T) + \frac{\partial}{\partial x}(c_p \rho T v) = \frac{\partial}{\partial x}\left(\lambda \frac{\partial T}{\partial x}\right) + \sum_i D_i \rho \frac{\partial h_i}{\partial x}\frac{\partial \omega_i}{\partial x} - \sum_i h_i \phi_i \tag{2}$$

$$\frac{\partial}{\partial t}(\rho \omega_i) + \frac{\partial}{\partial x}(\rho \omega_i v) = \frac{\partial}{\partial x}\left(D_i \rho \frac{\partial \omega_i}{\partial x}\right) + \phi_i \tag{3}$$

$$p = \rho R T \sum_i \frac{\omega_i}{m_i} \tag{4}$$

where ω_i and ϕ_i are, respectively, the mass fraction and the chemical production rate of the i-th species. The other symbols have their usual meanings.

The partial differential terms in the governing equations were transformed into the corresponding finite difference terms according to the control-volume method.[2)] The obtained finite-difference equations were solved numerically under the following boundary conditions; at the unburned side the temperature is 298 K and the combustible gas mixture is composed of the fuel and air, and at the burned side the gas is heated up to the adiabatic flame temperature, which is evaluated beforehand based on the combustion condition, and has the equilibrium composition at that temperature. The solutions individually converge to certain values independent of the initial condition only when the flow velocity given as one of the boundary conditions just agrees with the burning velocity which is the eigenvalue for the combustion condition.

Reaction Scheme for Methane Combustion

Methane combustion actually consists of a wide variety of elementary reactions including those occurring among C_2 and higher hydrocarbons, particularly when air is supplied insufficiently, because soot is produced under such conditions. Reaction schemes including higher hydrocarbons have been proposed[3–5)] and used for combustion of fuels containing eight or more carbon atoms in their molecules. Those schemes are, however, too complicated to be applied to methane combustion, though they should be employed when soot-formation processes, for example, are discussed.

In this investigation, we composed a reaction scheme comprising only C_1 and C_2 hydrocarbons (Table 1), and applied it to methane combustion under various conditions. Nitrogen works as the source of thermal NO_x in actual flames but in this investigation it is assumed to be inert due to the consideration of the production rate of NO_x.[1)] Most of the rate coefficients except those of

Table 1. CH_4–O_2 Reaction Scheme
$k=AT^n\exp(-E/T)$

No.	Reaction	A	n	E	Ref.
R1	$CH_4+M \rightarrow CH_3+H+M$	1.41E10	0.0	44500.0	6
R2	$CH_4+OH \rightarrow CH_3+H_2O$	3.47E-3	3.08	1010.0	6
R3	$CH_4+H \rightarrow CH_3+H_2$	2.20E-2	3.0	4400.0	7
R4	$CH_4+O \rightarrow CH_3+OH$	1.20E01	2.1	3840.0	7
R5	$CH_3+HO_2 \rightarrow CH_3O+OH$	3.24E07	0.0	0.0	6
R6	$CH_3+O_2 \rightarrow CH_3O+O$	2.51E07	0.0	14600.0	6
R7	$CH_3+OH \rightarrow HCHO+H_2$	3.98E06	0.0	0.0	6
R8	$CH_3+O \rightarrow HCHO+H$	7.00E07	0.0	0.0	7
R9	$CH_3+CH_3 \rightarrow C_2H_6$	4.00E06	0.0	0.0	6
R10	$CH_3+CH_3 \rightarrow C_2H_5+H$	8.00E07	0.0	13400.0	7
R11	$CH_3+CH_3 \rightarrow C_2H_4+H_2$	1.00E10	0.0	16100.0	7
R12	$CH_3O+O_2 \rightarrow HCHO+HO_2$	1.00E06	0.0	3020.0	6
R13	$CH_3O+M \rightarrow HCHO+H+M$	5.01E07	0.0	10600.0	6
R14	$HCHO+OH \rightarrow CHO+H_2O$	7.59E06	0.0	85.5	6
R15	$HCHO+H \rightarrow CHO+H_2$	3.31E08	0.0	5280.0	6
R16	$HCHO+O \rightarrow CHO+OH$	5.01E07	0.0	2310.0	6
R17	$HCHO+M \rightarrow CHO+H+M$	3.31E10	0.0	40800.0	6
R18	$CHO+OH \rightarrow CO+H_2O$	1.00E08	0.0	0.0	6
R19	$CHO+H \rightarrow CO+H_2$	2.00E08	0.0	0.0	6
R20	$CHO+O \rightarrow CO+OH$	1.00E08	0.0	0.0	6
R21	$CHO+O_2 \rightarrow CO+HO_2$	3.98E06	0.0	3520.0	6
R22	$CHO+M \rightarrow CO+H+M$	5.00E09	0.0	8460.0	7
R23	$CO+OH \rightarrow CO_2+H$	4.40E00	1.5	−373.0	7
R24	$CO+O+M \rightarrow CO_2+M$	5.89E03	0.0	2060.0	6
R25	$CO+HO_2 \rightarrow CO_2+OH$	1.51E08	0.0	11900.0	6
R26	$CO+O_2 \rightarrow CO_2+O$	3.16E05	0.0	18900.0	6
R27	$C_2H_6+OH \rightarrow C_2H_5+H_2O$	1.12E07	0.0	1230.0	6
R28	$C_2H_6+H \rightarrow C_2H_5+H_2$	5.37E-4	3.5	2620.0	6
R29	$C_2H_6+O \rightarrow C_2H_5+OH$	2.51E07	0.0	3200.0	6
R30	$C_2H_6+CH_3 \rightarrow C_2H_5+CH_4$	5.50E-7	4.0	4170.0	6
R31	$C_2H_5+O_2 \rightarrow C_2H_4+HO_2$	1.00E06	0.0	2520.0	6
R32	$C_2H_5+M \rightarrow C_2H_4+H+M$	2.00E09	0.0	15100.0	6
R33	$C_2H_4+OH \rightarrow C_2H_3+H_2O$	4.79E06	0.0	619.0	6
R34	$C_2H_4+H \rightarrow C_2H_3+H_2$	1.51E01	2.0	3020.0	6
R35	$C_2H_4+M \rightarrow C_2H_3+H+M$	6.31E12	0.0	54700.0	6
R36	$C_2H_4+M \rightarrow C_2H_2+H_2+M$	9.33E10	0.0	38800.0	6
R37	$C_2H_4+OH \rightarrow CH_3+HCHO$	2.00E06	0.0	483.0	6
R38	$C_2H_4+O \rightarrow CH_3+CHO$	3.31E06	0.0	569.0	6
R39	$C_2H_4+O \rightarrow HCHO+CH_2$	2.51E07	0.0	2520.0	6
R40	$C_2H_3+H \rightarrow C_2H_2+H_2$	2.00E07	0.0	1260.0	6
R41	$C_2H_3+O_2 \rightarrow C_2H_2+HO_2$	1.00E06	0.0	5030.0	6
R42	$C_2H_3+M \rightarrow C_2H_2+H+M$	7.94E08	0.0	15900.0	6
R43	$C_2H_2+OH \rightarrow C_2H+H_2O$	6.03E06	0.0	3520.0	6
R44	$C_2H_2+H \rightarrow C_2H+H_2$	2.00E08	0.0	9560.0	6
R45	$C_2H_2+O \rightarrow C_2H+OH$	3.24E09	−0.6	8550.0	6
R46	$C_2H_2+M \rightarrow C_2H+H+M$	1.00E08	0.0	57400.0	6
R47	$C_2H_2+OH \rightarrow CH_2CO+H$	3.24E05	0.0	101.0	6
R48	$C_2H_2+O \rightarrow HCCO+H$	3.55E-2	2.7	699.0	6
R49	$C_2H_2+O \rightarrow CH_2+CO$	6.76E07	0.0	2010.0	6
R50	$C_2H_2+O_2 \rightarrow CHO+CHO$	3.98E06	0.0	14100.0	6
R51	$C_2H+O_2 \rightarrow CHO+CO$	1.00E07	0.0	3520.0	6
R52	$C_2H+O \rightarrow CH+CO$	5.01E07	0.0	0.0	6
R53	$CH_2CO+OH \rightarrow HCCO+H_2O$	1.00E07	0.0	0.0	6
R54	$CH_2CO+H \rightarrow HCCO+H_2$	1.00E07	0.0	0.0	6
R55	$CH_2CO+O \rightarrow HCCO+OH$	1.00E07	0.0	0.0	6
R56	$CH_2CO+OH \rightarrow HCHO+CHO$	2.82E07	0.0	0.0	6
R57	$CH_2CO+H \rightarrow CH_3+CO$	1.10E07	0.0	1710.0	6
R58	$CH_2CO+O \rightarrow CHO+CHO$	1.00E07	0.0	1210.0	6
R59	$CH_2CO+M \rightarrow CH_2+CO+M$	2.00E10	0.0	30200.0	6
R60	$HCCO+OH \rightarrow CHO+CHO$	1.00E07	0.0	0.0	6
R61	$HCCO+H \rightarrow CH_2+CO$	5.01E07	0.0	0.0	6
R62	$HCCO+O \rightarrow CO+CHO$	3.39E07	0.0	1010.0	6
R63	$CH_2+OH \rightarrow CH+H_2O$	2.69E05	0.67	12900.0	6
R64	$CH_2+H \rightarrow CH+H_2$	2.69E05	0.67	12900.0	6

Table 1. (Continued)

No.	Reaction	*A*	*n*	*E*	Ref.
R65	$CH_2+O \rightarrow CH+OH$	1.91E05	0.68	12600.0	6
R66	$CH_2+O_2 \rightarrow CHO+OH$	1.00E08	0.0	1860.0	6
R67	$CH+O_2 \rightarrow CHO+O$	1.00E07	0.0	0.0	6
R68	$CH+O_2 \rightarrow CO+OH$	1.35E05	0.67	12900.0	6
R69	$H+O_2 \rightarrow OH+O$	2.20E08	0.0	8450.0	8
R70	$O+H_2 \rightarrow OH+H$	1.80E04	1.0	4480.0	8
R71	$OH+OH \rightarrow O+H_2O$	6.30E06	0.0	550.0	8
R72	$OH+H_2 \rightarrow H+H_2O$	2.20E07	0.0	2590.0	8
R73	$H+H+M \rightarrow H_2+M$	2.60E06	−1.0	0.0	8
R74	$O+O+M \rightarrow O_2+M$	1.90E01	0.0	−900.0	8
R75	$H+O+M \rightarrow OH+M$	3.60E06	−1.0	0.0	9
R76	$OH+H+M \rightarrow H_2O+M$	4.06E10	−2.0	0.0	8
R77	$H+O_2+M \rightarrow HO_2+M$	5.00E03	0.0	−500.0	8
R78	$H+HO_2 \rightarrow H_2+O_2$	2.50E07	0.0	350.0	8
R79	$H+HO_2 \rightarrow OH+OH$	2.50E08	0.0	950.0	8
R80	$H+HO_2 \rightarrow O+H_2O$	9.00E05	0.5	2000.0	8
R81	$OH+HO_2 \rightarrow H_2O+O_2$	5.00E07	0.0	500.0	9
R82	$O+HO_2 \rightarrow OH+O_2$	6.30E07	0.0	350.0	10

The rate constants are expressed in m, mol, s units.

hydrogen–oxygen reactions were selected from the values proposed by Westbrook[6] and Warnatz.[7] Some of the frequency factors, however, were modified to make the scheme applicable for combustion of methane under wide conditions and, in addition, for that of ethane, ethylene and acetylene under stoichiometric and lean conditions.

The thermal conductivities and diffusion coefficients of the component gases were evaluated as functions of temperature according to Eucken's and Hirschfelder's approximations,[12] respectively. The values of these properties for the gas mixtures were estimated by summation of the corresponding values of the individual components with multiplication by factors depending on the gas compositions.

Results and Discussion

Validity of Proposed Reaction Scheme. The calculated burning velocities of methane–air premixed flames with various equivalence ratios were compared with those obtained experimentally[13] (Fig. 1). The predicted burning velocities for stoichiometric ethane–, ethylene–, and acetylene–air flames were also checked with the experimental values (Table 2).

The burning velocity predicted by use of computer simulation is given as an overall result of interactions among chemical and physical processes constituting the model. Good agreement between the predicted and the experimental burning velocities leads to the conclusion that the model including the reaction scheme proposed in this investigation are valid for simulation of actual methane flames.

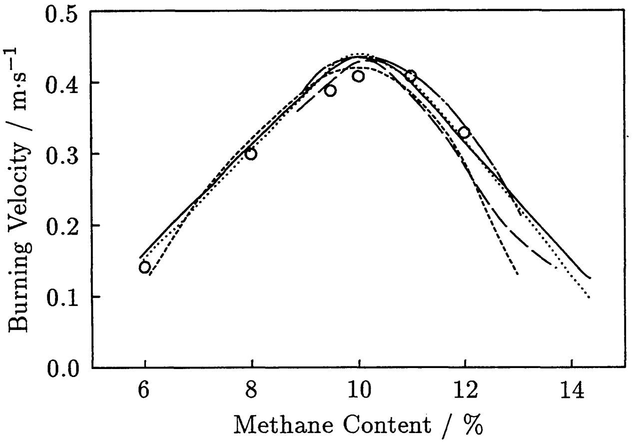

Fig. 1. Comparison of the predicted burning velocities (circles) with the experimental ones which were summarized by Andrews et al.[13]

Table 2. Stoichiometric Hydrocarbon-Air premixed Flames

Hydrocarbons	C_2H_2	C_2H_4	C_2H_6	CH_4
Buring velocity/m s^{-1}	1.56	0.76	0.49	0.39
Initial mole fraction of fuel/%	7.73	6.53	5.65	9.48
Adiabatic flame temperature/K	2550	2380	2260	2230
Experimental burning velocity[14]/m s^{-1}	1.56	0.78	0.48	0.42

Combustion Reaction in Stoichiometric Methane Flame. Figure 2 shows the profiles of the temperature and the mole fractions of stable species in a stoichiometric methane–air premixed flame. Water vapor, one of the final combustion products, is already present even at a very early stage; carbon dioxide, on the contrary, is not produced in a large amount until most methane has been consumed. These changes suggest that carbon and hydrogen contained in the fuel molecule are oxidized through different routes in methane combustion.

The mole-fraction profiles of active or intermediate

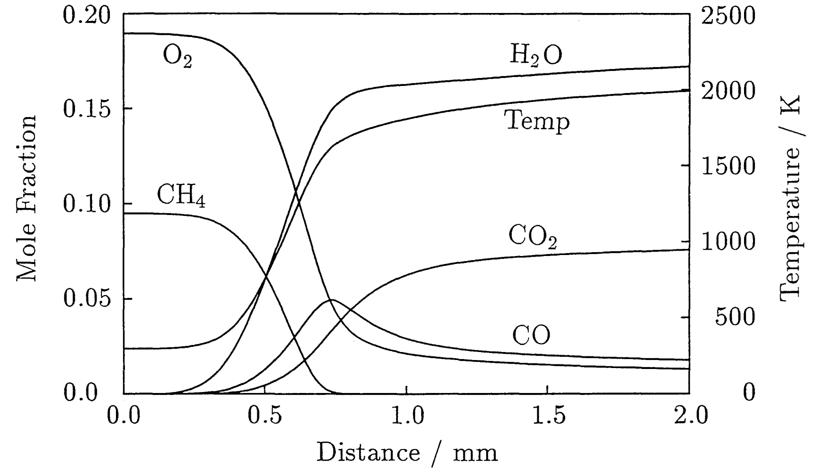

Fig. 2. Profiles of the temperature and the concentrations of stable species in a stoichiometric methane–air premixed flame.

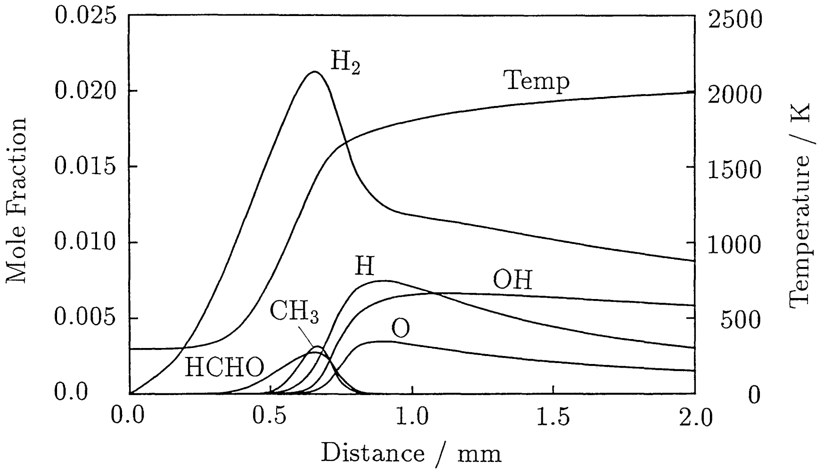

Fig. 3. Profiles of the temperature and the concentrations of active species in the stoichiometric methane–air premixed flame.

species are given in Fig. 3. The three active species, hydroxyl radicals and hydrogen and oxygen atoms, generally holding a decisive role in combustion, do not increase until the temperature becomes higher than 1000 K. These profiles are quite different from those in hydrogen premixed flames,[1] where hydrogen atoms diffusing from the flame front to the low-temperature region carry enthalpy as chemical energy, release it as thermal energy through reactions toward less active species, and raise temperature there.

Figure 4 shows the heat increase rates due to the four possible terms which appear in the conservation equation of thermal energy, Eq. 2, that is, convection, conduction, heat transfer accompanying species diffusion and heat release by chemical reactions. The condition that the summation of the above four contributions must be zero at any position in a steady flame is satisfied. Thermal energy is practically accumulated both by conduction and heat release at low temperatures but increases only by heat release at high temperatures. Species diffusion does not contribute to the transfer of thermal energy as also observed in hydrogen flames.

Temperature must be raised at any part of a flame for its steady propagation. It is easy to raise temperature in the high-temperature region because of the intense heat release through reactions, but is difficult in the low-temperature region;·therefore the mode how the temperature is raised there governs the propagation mechanism of the whole flame. Two theories have been proposed for the propagation mechanism of a premixed flame depending on which of the two factors, conduction and heat release, is considered to be responsible for the thermal energy increase in its low-temperature region;[15] the thermal propagation theory, which assumes that the former is predominant, and the active-species diffusion theory, which is constructed on the mechanism that active species diffuse to the low-temperature region from the flame front and are degraded to stable species through exothermic reactions. In the latter theory the active species can be considered to be hydrogen atoms

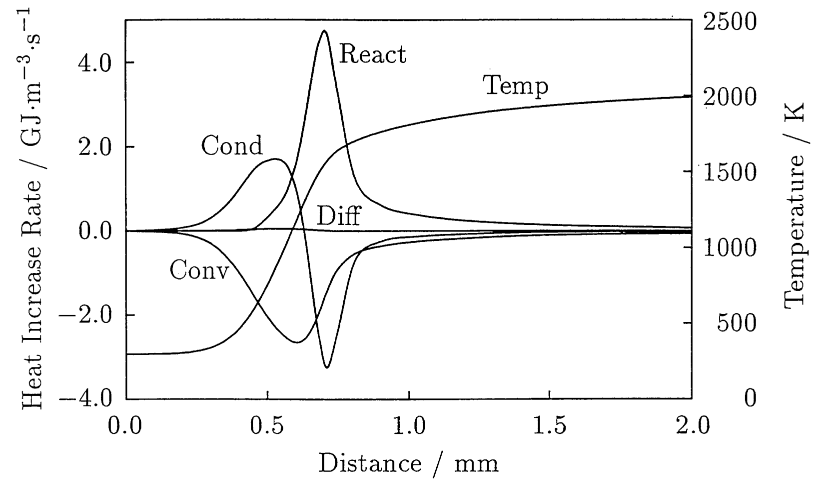

Fig. 4. Rates of the heat increase due to convection (Conv), conduction (Cond), heat transfer accompanying species diffusion (Diff), and heat release through reactions (React) in the stoichiometric methane–air premixed flame.

without substantial error because of their large diffusion coefficient. In the stoichiometric methane–air premixed flame, chemical reactions do not release yet thermal energy in a large amount at low temperatures as shown in Fig. 4, suggesting that this flame is a typical example of thermally-propagating flames.

We now discuss the reasons why the methane flame propagates thermally.

One of the characteristics of the distribution of heat-release rate in the methane flame is that heat is evolved at fairly high temperatures comparing with that in a stoichiometric hydrogen-air flame;[1] the contribution of heat release in the methane flame increases at about 1000K, equals that of conduction at 1120K, and decreases steeply after reaching its maximum at 1550K, while in the hydrogen flame it becomes significant already at about 400K and exceeds the thermal conduction at 450K. This comparison between these changes in the heat-release profiles suggests that initiation of the combustion reaction is retarded in the methane flame.

According to simulation of methane premixed flames, the main combustion reactions proceed sequentially as $CH_4 \rightarrow CH_3 \rightarrow HCHO \rightarrow CHO \rightarrow CO \rightarrow CO_2$ under stoichiometric or lean conditions.[7] At 1550 K in the stoichiometric flame, the reaction pathways are shown in Fig. 5 and the predominant reactions for each step are:

$$CH_4 + OH \rightarrow CH_3 + H_2O, \quad (R2)$$

$$CH_4 + H \rightarrow CH_3 + H_2; \quad (R3)$$

$$CH_3 + O \rightarrow HCHO + H; \quad (R8)$$

$$HCHO + H \rightarrow CHO + H_2, \quad (R15)$$

$$HCHO + OH \rightarrow CHO + H_2O; \quad (R14)$$

$$CHO + M \rightarrow CO + H + M. \quad (R22)$$

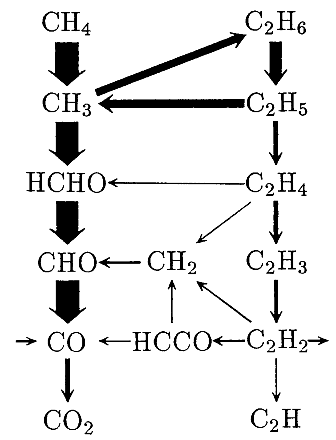

Fig. 5. Reaction pathways at 1550 K in the stoichiometric methane flame. The widths of the arrows are proportional to the rates of the corresponding reactions.

The contributions of reactions (R2) and (R3) are, respectively, 55% and 37% for the total methane dehydrogenation; 88% of the methyl oxidation is ascribed to reaction (R8); 63% and 22% of formyl radicals are produced by reactions (R15) and (R14), respectively; almost all formyl radicals are decomposed to carbon monoxide by reaction (R22).

About 85% of the carbon monoxide cannot be oxidized yet into carbon dioxide even at this temperature. Its oxidation is activated only after the fuel has been exhausted. Almost all carbon monoxide reacts with hydroxyl radicals via reaction

$$CO + OH \rightarrow CO_2 + H. \quad (R23)$$

The slow oxidation of carbon monoxide is explained as follows. There are several reactions consuming hydroxyl radicals such as reactions (R2), (R72), (R14), and

(R23) at high temperatures. The oxidation step of carbon monoxide, however, has the smallest rate constant among them, though it has a negative activation temperature (see Table 1). It can be activated for the first time after all the other consumption reactions of hydroxyl radicals have actually been completed.

Methoxyl radicals are present at low temperatures. At 1120 K, where the rates of heat increase due to conduction and heat release are equal, for instance, about 40% of the methyl radicals are once oxidized to methoxyl radicals via reaction

$$CH_3 + HO_2 \rightarrow CH_3O + OH. \qquad (R5)$$

These radicals are further decomposed through reactions

$$CH_3O + M \rightarrow HCHO + H + M \qquad (R13)$$

and

$$CH_3O + O_2 \rightarrow HCHO + HO_2, \qquad (R12)$$

in the stoichiometric flame. The rest of the methyl radicals are oxidized through reaction (R8). The direct oxidation of methyl to formaldehyde increases with increasing temperature.

A chemical process composed of a sequence of elementary reactions cannot proceed as a whole when any step is delayed. The oxidation step of methyl radicals is mostly due to reaction (R8); therefore oxygen atoms must be present for smooth progression of methane combustion. That species, however, cannot be supplied by diffusion because of its small diffusion coefficient. Hence they must be inevitably supplied by reactions.

Oxygen atoms are produced mostly through a chain-branching reaction

$$H + O_2 \rightarrow OH + O \qquad (R69)$$

over a wide range of temperature. As shown in Table 1, this reaction is competing with reaction

$$H + O_2 + M \rightarrow HO_2 + M. \qquad (R77)$$

Reaction (R77) is activated in a low-temperature region because of its negative activation energy, so that reaction (R69) becomes faster than reaction (R77) at temperatures as high as 1100K; in other words, oxygen atoms cannot be produced in a sufficient amount and, hence, the whole combustion reaction of methane cannot be accelerated at low temperatures. This is the main reason why methane flames propagate thermally, and has been also confirmed by experiments.[16)]

The propagation mechanism of a premixed flame is also controlled by the possibility of efficient formation of free hydrogen atoms; when they are sufficiently produced in a flame its propagation can be explained according to the active-species diffusion theory. Hydrogen atoms initially contained in methane molecules are finally oxidized into water molecules via several kinds of species. The number of hydrogen atoms shared in the fuel decreases almost linearly with rising temperature and instead that shared in water vapor increases, and the number of hydrogen atoms contained in hydrogen molecules is kept around 10% throughout the whole temperature range. The stable final product is directly produced from the fuel at the first step of the combustion, that is, reaction (R2), and holds about half of the hydrogen atoms at temperature as low as 1000 K; thus free hydrogen atoms cannot be appreciably liberated until complete consumption of the fuel.

Heat release due to chemical reactions is caused predominantly by the following reactions: reaction (R1) at low temperatures, reaction (R9) at 950—1300 K, reaction (R8) at 1400—1650 K, reaction (R23) at 1700—1800 K, and reactions (R76) and (R77) at higher temperatures. The contribution of reaction (R8) is the most important; the fairly steep decrease in the heat-release rate after passing its maximum as shown in Fig. 4 is ascribable to the decrease in the rate of this reaction. It is noteworthy that reaction

$$CH_4 + M \rightarrow CH_3 + H + M \qquad (R1)$$

proceeds in the reverse direction and release a remarkable amount of thermal energy in a low-temperature region, though this reaction is generally considered to be one of the initiation reactions. The rate constant of its reverse reaction must be exactly evaluated from the viewpoint of the heat release at low temperatures.

Combustion Reactions under Various Conditions and Role of C_2 Routes. The combustion reactions in methane–air premixed flames proceed in various mechanisms depending on their initial fuel concentrations. The reaction paths via C_2 hydrocarbons are not important under the stoichiometric condition as described above though its contribution is not negligible. They are, however, of importance as a combustion route and also a starting step of soot formation under rich conditions. We simulated five other methane flames with various equivalence ratios and carried out a comparative study of their reaction mechanisms.

The equivalence ratios of the additional flames are 1.30, 1.18, 1.06, 0.83, and 0.61, and the calculated burning velocities are 0.33, 0.41, 0.41, 0.30, and 0.14 m s^{-1}, respectively. These velocities are in good agreement with the corresponding experimental values as shown in Fig. 1.

As the equivalence ratio increases, the oxidation of carbon monoxide is naturally suppressed and a larger amount of carbon monoxide is left unburned even at the adiabatic flame temperature. More than 5% of the carbon atoms are, however, contained temporarily in the C_2 hydrocarbons even in the flame with the equivalence ratio of 0.61, and the maximum ratio of the carbon atoms shared in the C_2 hydrocarbons monotonically increases with the increasing equivalence ratio reaching about 14%

in the richest flame among those investigated here; the temperature where the maximum ratio is achieved ranges from 1100K (at the leanest condition) to 1360K (at the richest one).

We estimated the roles of the C_2 routes from chemical viewpoints.

Some of methyl radicals are recombined to ethane through reaction

$$CH_3 + CH_3 \rightarrow C_2H_6, \qquad \text{(R9)}$$

and the ethane is predominantly dehydrogenated through

$$C_2H_6 + H \rightarrow C_2H_5 + H_2 \qquad \text{(R28)}$$

and

$$C_2H_6 + OH \rightarrow C_2H_5 + H_2O \qquad \text{(R27)}$$

in all the flames throughout wide ranges of temperature. It should be noted that more than half of the ethyl radicals dissociate again into methyl radicals by the reaction with hydrogen atoms:

$$C_2H_5 + H \rightarrow CH_3 + CH_3 \qquad \text{(R10)}$$

In other words, the C_2 routes partly work just as a temporary storage of the carbon-containing species and, in addition, as radical-consuming steps for methane combustion. Therefore, we evaluated the net roles of the C_2 routes by use of the ratio between the amounts of methyl radicals reacting to methoxyl or formaldehyde and that of ethyl radicals reacting to ethylene. Figure 6 shows those ratios in the stoichiometric and rich flames as functions of temperature. According to this figure, the ratios become minimum at around 1200 K in both flames indicating that the relative importance of the C_2 routes are almost similar as a whole independently of the equivalence ratio and also are remarkable at low temperatures.

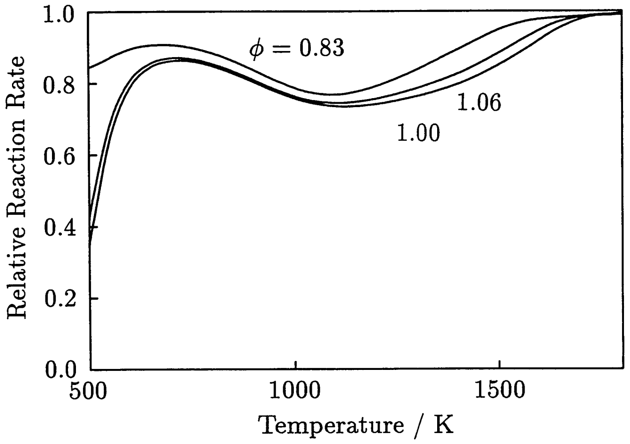

Fig. 6. Relative reaction rates of the C_1 and the C_2 routes in the three methane flames depicted with the equivalence ratio.

About 40% of the ethyl radicals further react as C_2 species. In all the flames simulated in this investigation, the C_2 routes starting from ethyl radicals progress predominantly as $C_2H_5 \rightarrow C_2H_4 \rightarrow C_2H_3 \rightarrow C_2H_2$ though there are some side pathways (see Fig. 5); acetylene is consequently produced through the sequence of reactions

$$C_2H_5 + M \rightarrow C_2H_4 + H + M; \qquad \text{(R32)}$$

$$C_2H_4 + H \rightarrow C_2H_3 + H_2, \qquad \text{(R34)}$$

$$C_2H_4 + OH \rightarrow C_2H_3 + H_2O; \qquad \text{(R33)}$$

$$C_2H_3 + H \rightarrow C_2H_2 + H_2, \qquad \text{(R40)}$$

$$C_2H_3 + M \rightarrow C_2H_2 + H + M. \qquad \text{(R42)}$$

The contribution of reaction (R32) for the first step is more than 90% at 1550 K in the stoichiometric flame, for instance; those of reactions (R34) and (R33) for the dehydrogenation of ethylene are 73% and 27%, respectively; about 52% and 44% of acetylene is produced through reactions (R40) and (R42), respectively.

More than 80% of the acetylene is oxidized with oxygen atoms by either of the following two reactions, which have almost the same contributions in the above-mentioned flame:

$$C_2H_2 + O \rightarrow HCCO + H \qquad \text{(R48)}$$

$$C_2H_2 + O \rightarrow CH_2 + CO. \qquad \text{(R49)}$$

The rest of the acetylene is further dehydrogenated through reactions

$$C_2H_2 + H \rightarrow C_2H + H_2 \qquad \text{(R44)}$$

and

$$C_2H_2 + OH \rightarrow C_2H + H_2O. \qquad \text{(R43)}$$

Application of Simple Reaction Scheme. The reaction paths through C_2 hydrocarbons are not major routes of methane combustion at least under the stoichiometric and lean conditions. Therefore, some combustion phenomena particularly in real flames have been investigated applying simplified reaction schemes to avoid complexities; reaction schemes which are composed of only three or four reactions have been proposed,[17,18] for instance.

Those schemes are useful for confined purposed such as general surveys of combustion reactions in flames having complicated flow fields and discussion in considering chemical reactions only as heat-releasing processes. But they are too simple and, furthermore, are not necessarily composed of so-called elementary reactions; they are not satisfactory at least for the analyses of reaction mechanisms of combustion. Here we made a simple reaction scheme which is composed of C_1 hydrocarbon elementary reactions and, at the same time, is exact enough to reproduce methane combustion reactions, though they can only be applied for combustion under stoichiometric and lean conditions. The simple reaction scheme is also expected to elucidate the importance of the C_2 routes in comparison with the results obtained by use of the full and the simple reaction schemes.

The proposed simple reaction scheme consists in thirtyseven pairs of elementary reactions (Table 3). At first, we assumed the same rate coefficients, that is, *A*, *n*, and *E*, as those in Table 1 for each reaction of the simple scheme. However, the predicted burning velocity of the stoichiometric methane flame, for example, was as large as $0.49\,\mathrm{ms}^{-1}$, while both burning velocities obtained by experiments and predicted with the full reaction scheme are around $0.4\,\mathrm{ms}^{-1}$.

An elementary reaction should universally have the same rate coefficients independently of what reaction scheme it belongs to. This principle, however, is strictly followed only when the reaction is a constituent of a complete scheme. On the contrary, when it belongs to an abbreviated scheme, its rate coefficients may be modified to compensate the influences coming from the omission of reactions, though the omitted reactions individually have only negligible effects on the whole combustion process. A trial and error method led to the

Table 3. Simple CH_4–O_2 Reaction Scheme
$k=AT^n\exp(-E/T)$

No.	Reaction	*A*	*n*	*E*
R1	$CH_4+M\rightarrow CH_3+H+M$	1.41E10	0.0	44500
R2	$CH_4+OH\rightarrow CH_3+H_2O$	3.47E-3	3.08	1010
R3	$CH_4+H\rightarrow CH_3+H_2$	2.20E-2	3.0	4400
R4	$CH_4+O\rightarrow CH_3+OH$	1.20E01	2.1	3840
R5	$CH_3+HO_2\rightarrow CH_3O+OH$	3.24E07	0.0	0
R6	$CH_3+O_2\rightarrow CH_3O+O$	2.51E07	0.0	14600
R7	$CH_3+OH\rightarrow HCHO+H_2$	3.98E06	0.0	0
R8	$CH_3+O\rightarrow HCHO+H$	7.00E07	0.0	0
R9	$CH_3O+O_2\rightarrow HCHO+HO_2$	1.00E06	0.0	3020
R10	$CH_3O+M\rightarrow HCHO+H+M$	5.01E07	0.0	10600
R11	$HCHO+OH\rightarrow CHO+H_2O$	7.59E06	0.0	85.5
R12	$HCHO+H\rightarrow CHO+H_2$	3.31E08	0.0	5280
R13	$HCHO+O\rightarrow CHO+OH$	5.01E07	0.0	2310
R14	$HCHO+M\rightarrow CHO+H+M$	3.31E10	0.0	40800
R15	$CHO+OH\rightarrow CO+H_2O$	1.00E08	0.0	0
R16	$CHO+H\rightarrow CO+H_2$	2.00E08	0.0	0
R17	$CHO+O\rightarrow CO+OH$	1.00E08	0.0	0
R18	$CHO+O_2\rightarrow CO+HO_2$	3.98E06	0.0	3520
R19	$CHO+M\rightarrow CO+H+M$	1.42E09	0.0	8460
R20	$CO+OH\rightarrow CO_2+H$	4.40E00	1.5	−373
R21	$CO+O+M\rightarrow CO_2+M$	5.89E03	0.0	2060
R22	$CO+HO_2\rightarrow CO_2+OH$	1.51E08	0.0	11900
R23	$CO+O_2\rightarrow CO_2+O$	3.16E05	0.0	18900
R24	$H+O_2\rightarrow OH+O$	1.20E11	−0.91	8310
R25	$O+H_2\rightarrow OH+H$	1.80E04	0.0	4480
R26	$OH+OH\rightarrow O+H_2O$	6.30E06	0.0	550
R27	$OH+H_2\rightarrow H+H_2O$	2.20E07	0.0	2590
R28	$H+H+M\rightarrow H_2+M$	2.60E06	−1.0	0
R29	$O+O+M\rightarrow O_2+M$	1.90E01	0.0	−900
R30	$H+O+M\rightarrow OH+M$	3.60E06	−1.0	0
R31	$OH+H+M\rightarrow H_2O+M$	4.06E10	−2.0	0
R32	$H+O_2+M\rightarrow HO_2+M$	5.00E03	0.0	−500
R33	$H+HO_2\rightarrow H_2+O_2$	2.50E07	0.0	350
R34	$H+HO_2\rightarrow OH+OH$	2.50E08	0.0	950
R35	$H+HO_2\rightarrow O+H_2O$	9.00E05	0.5	2000
R36	$OH+HO_2\rightarrow H_2O+O_2$	5.00E07	0.0	500
R37	$O+HO_2\rightarrow OH+O_2$	6.30E07	0.0	350

The rate constants are expressed in m, mol, s units.

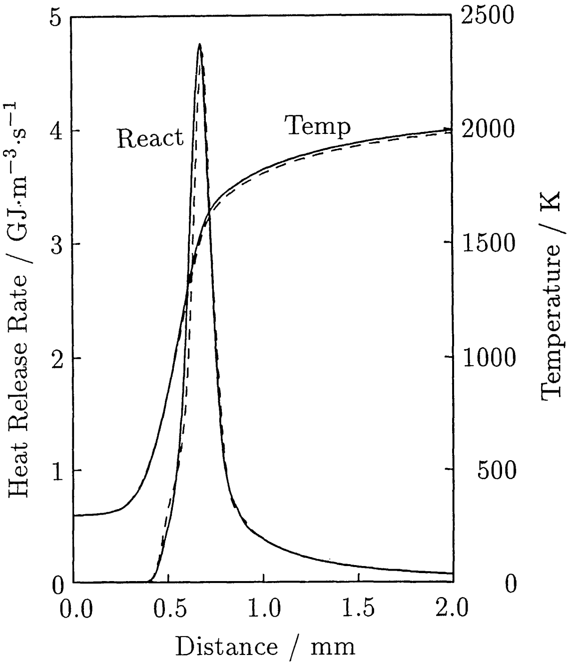

Fig. 7. Comparison of the temperature and the heat-release rate predicted by use of the C_2 scheme (solid lines) and the C_1 scheme (dashed lines).

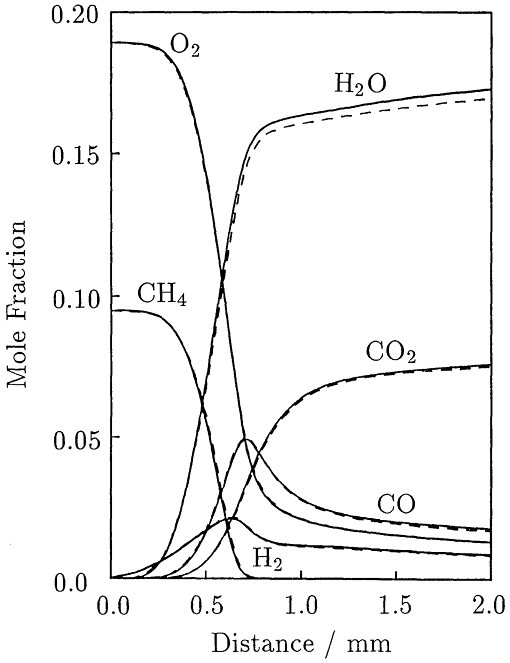

Fig. 8. Comparison of the concentrations of the stable species predicted by use of the C_2 scheme (solid lines) and the C_1 scheme (dashed lines).

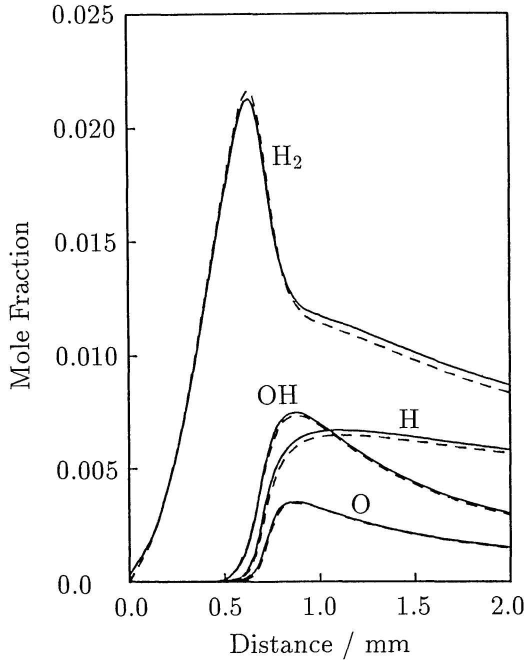

Fig. 9. Comparison of the concentrations of the intermediate species predicted by use of the C_2 scheme (solid lines) and the C_1 scheme (dashed lines).

result that multiplication of the frequency factor of reaction (R22) in Table 1 by a factor of 0.284 is the most suitable modification. The routes via the C_2 hydrocarbons are, therefore, approximately equivalent to the suppression of the rate of the sequential oxidation of methane via the C_1 hydrocarbons. In other words, those routes have inhibiting effects on methane combustion.

Then, the burning velocity was improved to be 0.38 m s^{-1} for the stoichiometric methane flame. Figure 7 shows the profiles of the temperature and the heat-release rate of the stoichiometric methane flame calculated by using both reaction schemes. Figures 8 and 9 designate the mole-fraction profiles of the stable and active or intermediate species, respectively. These profiles are in good agreement except those of water and hydrogen. The number of the carbon atoms shared in the other species except methane, carbon monoxide and carbon dioxide obtained by means of the C_2-hydrocarbon scheme is about 1.5 times as large as that calculated by using the C_1-hydrocarbon reaction scheme.

Conclusions

Two reaction schemes for combustion reactions of C_1 and C_2 hydrocarbons were proposed and applied to flat premixed methane flames. The following conclusions were obtained:

1. Methane combustion proceeds predominantly via the C_1 routes under stoichiometric and lean conditions; the C_2 routes hold only a subordinate role. However the omission of the C_2 routes from the reaction scheme causes increase in the burning velocity because they work as a temporary storage of the species. The rate constant of reaction (R22) should be reduced to compensate the unreasonable raise of the burning velocity in a simplified reaction scheme which comprises only the C_1 routes.
2. A methane premixed flame propagates mainly according to the thermal theory, which is applicable to the propagation of flames where reactions do not occur in the low-temperature regions, because methane combustion reactions have not been activated until the temperature is raised up to about 1100 K; the oxidation of methyl radicals inevitably requires oxygen atoms but these cannot be supplied at lower temperatures due to a competition reaction for their formation.

References

1) S. Fukutani, N. Kunioshi, and H. Jinno, *Bull. Chem. Soc. Jpn.,* **63**, 2191 (1990).

2) S. V. Patankar, "Numerical Heat Transfer and Fluid Flow," Hemisphere Publishing Co., New York (1980), Chap. 3.

3) J. Warnatz, "Combustion Chemistry," ed by W. C. Gardiner, Jr., Springer-Verlag, New York (1984), pp. 197—360.

4) C. K. Westbrook, J. Creighton, C. Lund, and F. L. Dryer, *J. Phys. Chem.,* **81**, 2542 (1977).

5) P. Dagaut, M. Cathonnet, J. C. Boettner, and F. Gaillard, *Combust. Flame,* **71**, 295 (1988).

6) C. K. Westbrook, F. L. Dryer, and K. P. Schug, *Combust. Flame,* **52**, 299 (1983).

7) J. Warnatz, H. Bockhorn, A. Möser, and H. W. Wenz, "Nineteenth Symposium (International) on Combustion," The Combustion Institute, Pittsburgh (1982), pp. 197—209.

8) D. L. Baulch, D. D. Drysdale, D. G. Horne, and A. C. Lloyd, "Evaluated Kinetic Data for High Temperature Reactions," Butterworths, London (1972), Vol. 1.

9) D. E. Jensen and G. A. Jones, *Combust. Flame,* **32**, 1 (1978).

10) M. P. Heap, T. J. Tyson, J. E. Cichanowicz, R. Gershman, C. J. Kau, G. B. Martin, and W. S. Lanier, "Sixteenth Symposium (International) on Combustion," The Combustion Institute, Pittsburgh (1977), pp. 535—545.

11) D. L. Baulch, D. D. Drysdale, J. Duxbury, and S. Grant, "Evaluated Kinetic Data for High Temperature Reactions," Butterworths, London (1976), Vol. 3.

12) R. H. Perry and C. H. Chilton, "Chemical Engineer's Handbook," 5th ed, McGraw-Hill, New York (1973).

13) G. E. Andrews and D. Bradley, *Combust. Flame,* **20**, 77 (1973).

14) R. Günther and G. Janische, *Chemi. -Ing.-Tech.,* **43**, 975 (1971).

15) A. G. Gaydon and H. G. Wolfhard, "Flames," 4th ed, Chapman and Hall, London (1979), Chap. 5.

16) S. Fukutani, T. Sasaki, and H. Jinno, *Nenryo Kyokai Shi,* **69**, 946 (1990).

17) G. Paczko, P. M. Lefdal, and N. Peters, "Twenty-first Symposium (International) on Combustion," The Combustion Institute, Pittsburgh (1986), pp. 739—748.

18) N. Peters and F. A. Williams, *Combust. Flame,* **68**, 185 (1987).